Environmental Research Letters

ACCEPTED MANUSCRIPT • OPEN ACCESS

The global and regional impacts of climate change under Representative Concentration Pathway forcings and Shared Socioeconomic Pathway socioeconomic scenarios

To cite this article before publication: Nigel Arnell *et al* 2019 *Environ. Res. Lett.* in press https://doi.org/10.1088/1748-9326/ab35a6

Manuscript version: Accepted Manuscript

Accepted Manuscript is "the version of the article accepted for publication including all changes made as a result of the peer review process, and which may also include the addition to the article by IOP Publishing of a header, an article ID, a cover sheet and/or an 'Accepted Manuscript' watermark, but excluding any other editing, typesetting or other changes made by IOP Publishing and/or its licensors"

This Accepted Manuscript is **© 2019 The Author(s). Published by IOP Publishing Ltd**.

As the Version of Record of this article is going to be / has been published on a gold open access basis under a CC BY 3.0 licence, this Accepted Manuscript is available for reuse under a CC BY 3.0 licence immediately.

Everyone is permitted to use all or part of the original content in this article, provided that they adhere to all the terms of the licence https://creativecommons.org/licences/by/3.0

Although reasonable endeavours have been taken to obtain all necessary permissions from third parties to include their copyrighted content within this article, their full citation and copyright line may not be present in this Accepted Manuscript version. Before using any content from this article, please refer to the Version of Record on IOPscience once published for full citation and copyright details, as permissions may be required. All third party content is fully copyright protected and is not published on a gold open access basis under a CC BY licence, unless that is specifically stated in the figure caption in the Version of Record.

View the article online for updates and enhancements.

This content was downloaded from IP address 139.222.162.213 on 06/08/2019 at 09:18

The global and regional impacts of climate change under Representative Concentration Pathway forcings and Shared Socioeconomic Pathway socioeconomic scenarios

N. W. Arnell[1,7], J. A. Lowe[2,3], D. Bernie[2], R.J. Nicholls[4], S. Brown[4,5], A.J. Challinor[3] & T.J. Osborn[6]

[1] Department of Meteorology, University of Reading, UK

[2] Met Office Hadley Centre, Exeter, UK

[3] Priestley Centre, University of Leeds, UK

[4] Engineering and the Environment, University of Southampton, UK

[5] Department of Life and Environmental Sciences, Faculty of Science and Technology, Bournemouth University, UK

[6] Climatic Research Unit, School of Environmental Science, University of East Anglia, UK

[7] Author to whom any correspondence should be addressed

E-mail: n.w.arnell@reading.ac.uk

Keywords:
Climate change, hazard, impact, drought, flood, heatwave, agricultural impacts, ScenarioMIP, Shared Socioeconomic Pathways

Abstract

This paper presents an evaluation of the global and regional consequences of climate change for heat extremes, water resources, river and coastal flooding, droughts, agriculture and energy use. It presents change in hazard and resource base under different rates of climate change (Representative Concentration Pathways: RCP), and socio-economic impacts are estimated for each combination of RCP and Shared Socioeconomic Pathway. Uncertainty in the regional pattern of climate change is characterised by CMIP5 climate model projections. The analysis adopts a novel approach using relationships between level of warming and impact to rapidly estimate impacts under any climate forcing. The projections provided here can be used to inform assessments of the implications of climate change.

At the global scale all the consequences of climate change considered here are adverse, with large increases under the highest rates of warming. Under the highest forcing the global average annual chance of a major heatwave increases from 5% now to 97% in 2100, the average proportion of time in drought increases from 7% to 27%, and the average chance of the current 50-year flood increases from 2% to 7%. The socio-economic impacts of these climate changes are determined by socio-economic scenario. There is variability in impact across regions, reflecting variability in projected changes in precipitation and temperature.

The range in the estimated impacts can be large, due to uncertainty in future emissions and future socio-economic conditions and scientific uncertainty in how climate changes in response to future emissions. For the temperature-based indicators, the largest source of scientific uncertainty is in the estimated magnitude of equilibrium climate sensitivity, but for the indicators determined by precipitation the largest source is in the estimated spatial and seasonal pattern of changes in precipitation. By 2100 the range across socio-economic scenario is often greater than the range across the forcing levels.

Accepted Manuscript

1. Introduction

This paper presents a multi-sectoral analysis of the global and regional impacts of climate change through the 21st century, using a set of indicators that are directly relevant to policymakers at national and international scales calculated using consistent climate and socio-economic projections. It uses climate pathways representing seven levels of forcing describing different emissions pathways defined by Representative Concentration Pathways (O'Neill et al., 2016), together with five socio-economic scenarios representing future exposure defined by Shared Socioeconomic Pathways (SSPs: O'Neill et al., 2017). Scientific uncertainty in the translation of emissions forcing to change in regional climate is represented by (i) uncertainty in the estimated change in global mean temperature as estimated by the MAGICC energy balance model, and (ii) uncertainty in the spatial variability in relevant climate variables as characterised by 23 climate models.

The study uses around 20 indicators characterising impacts on heat extremes, water resources, river and coastal flooding, agriculture and energy use. It distinguishes explicitly between changes in the physical hazard and resource base – which are dependent on climate change – and socio-economic impacts which are a function of both change in climate and change in exposure. The paper uses a novel approach using relationships between level of warming (or sea level) and impact derived from spatially-explicit impacts models, which are then combined with probabilistic projections of increase in global mean temperature to rapidly estimate impacts under a wide range of alternative climate forcings. Whilst other studies have developed relationships between level of forcing and impact (e.g. Arnell et al., 2016a; Schleussner et al., 2016; Senivaratne et al., 2016; Arnell et al., 2019), this is the first time that such relationships have been combined with probabilistic temperature projections to estimate impacts under different forcings.

The analysis develops on earlier work (Arnell et al., 2013; 2016b; 2019), and uses more up-to-date climate pathways, climate models and socio-economic scenarios, probabilistic projections of global temperature change, and additional indicators that characterise a wider range of hazards and impacts. This paper presents summary charts of global and continental impacts, whilst more comprehensive regional tables and charts are presented in Supplementary Material. It does not itself explicitly assess or compare impacts across sectors and regions or describe in detail all impacts in all regions: such an assessment requires an explicit judgment of the relative importance of different indicators and thresholds defining 'significant' change. However, it provides regional information which will be directly relevant to such assessments, including those made in the forthcoming IPCC 6th Assessment Report. For example, the quantitative indicators can be grouped into 'severity classes' based on explicit thresholds, as is widely done in national risk assessments. The projected quantitative indicators of impact can also be combined with the qualitative characterisations of drivers of future vulnerability (for example as represented in the SSPs: O'Neill et al., 2017) to produce more nuanced narrative storylines suitable for stress testing or strategic evaluations.

In recent years an increasing number of studies have assessed the global scale impacts of climate change. Most of these have concentrated on individual sectors, including heat extremes (e.g. Tebaldi & Wehner, 2018; Lehner et al., 2018; Harrington et al., 2018, Dosio et al., 2018), drought (Smirnov et al., 2016; Naumann et al., 2018), flooding (Alfieri et al., 2017; Winsemius et al., 2016; Arnell & Gosling, 2016), water resources (Arnell & Lloyd-Hughes, 2014; Gosling & Arnell, 2016) and agriculture (e.g. Tebaldi & Lobell, 2018; Ruane et al., 2018; Schleussner et al., 2018). A small number have considered multiple impacts across sectors (e.g. Arnell et al., 2016b; Schleussner et al., 2016; O'Neill et al., 2018; Betts et al., 2018; Byers et al., 2018). Studies have used different climate pathways, including Representative Concentration Pathway (RCP) forcings and pathways consistent

Accepted Manuscript

with 1.5 and 2°C climate targets, and have used different sets of climate models to define climate scenarios.

2. Methods

2.1 Overview of approach

Scenario-based climate change impact studies typically estimate impacts from climate scenarios constructed from climate model simulations, and these impacts are therefore conditional on the forcings (such as Representative Concentration Pathways) used to run the climate models. However, not all climate models are run with all RCP forcings (and forcing scenarios can be updated), and users may be interested in impacts under different rates of forcing. This study uses 'damage functions' relating impacts (Section 2.2) in a given year to a simple metric of climate change (global mean surface temperature or increase in sea-level rise) together with projections of this metric under a defined level of forcing to estimate impacts over time (**Figure 1**). The different damage functions (left panel) represent uncertainty in the spatial pattern of change in climate variables, and the distribution of change in temperature in a given year (middle panel) represents the effects of uncertainty in the climate system parameters driving response to forcing (Section 2.5).

The damage functions are constructed 'bottom-up' using spatially-explicit impact models run with scenarios representing specific changes in global mean surface temperature or sea level. The damage functions for the socio-economic indicators are contingent on socio-economic scenario (Section 2.3) and therefore time. In this application, the damage functions are used to estimate impacts under the latest set of Representative Concentration Pathway forcings defined in ScenarioMIP (O'Neill et al., 2016), although in principle could be used with any temperature trajectories. There are some similarities with the (independently-developed) method used by Hsiang et al. (2017) to estimate economic impacts in the USA, although the details are different: most significantly the damage functions used in the current study take into account the spatial variability in change in climate as represented by the 23 CMIP5 climate model patterns.

It is assumed that each socio-economic scenario can be combined with each level of climate forcing (van Vuuren et al., 2014), although in practice high levels of forcing may not be plausible with some socio-economic scenarios and achieving low levels of forcing will be much more challenging under some than others (Riahi et al., 2017).

The period 1981-2010 is used to represent the reference climate against which the effects of climate change can be compared (the reference period sea level is the average over 1986-2005).

2.2 Indicators of impact

Table 1 summarises the indicators of hazard, resource base and impact, and specific definitions and details of their calculation are given in Supplementary Material. In each case, there are several plausible alternative indicators, and indeed each global impact study tends to use a different set of indicators for each area of impact. The indicators can be interpreted as proxies for change in hazard and impact. The hazard and resource indicators are expressed in physical terms (such as likelihood of occurrence of a specific magnitude event), and – with two exceptions – represent the regional average value of the indicator at a point (the two exceptions are the indicators calculating the regional area exposed to a significant change in river runoff and the area below the coastal 100-year flood level). The regional average agri-climate hazard indicators are calculated by weighting by

Accepted Manuscript

cropland areas. The other regional average hazard indicators are calculated by weighting by grid cell area, excluding grid cells with fewer than 1000 people in 2010. This weighting is used because the focus here is on the consequences of climate change relevant to people.

The impact indicators are all expressed as regional aggregations of numbers of people, area of cropland or energy use. The socio-economic indicators depend on socio-economic scenario, and indicators are calculated for each combination of socio-economic scenario and climate forcing.

The two heatwave magnitude indicators (defining heatwaves as either two or more days with temperatures greater than the 98th percentile of reference period warm-season temperatures, or four or more days with temperatures greater than the 99th percentile) represent different size heatwaves, one which currently has a 33% chance (approximately) of occurring in a place, and the other a 5% chance. The indicators based on average annual runoff represent pervasive water resources scarcity, whilst the indicators based on hydrological drought represent short-term availability. Similarly, the agricultural drought indicator represents short-term challenges to crop production in general. The change in crop growth duration is a proxy for crop yield (a shorter duration for crop growth is associated with reductions in yield: Challinor et al., 2016), and the crop heat stress indicator represents the effect of extreme events on yield (Gourdji et al., 2013). River flood hazard characterised by the annual likelihood of the reference period 50-year (2%) flood, and coastal flood hazard is represented by the area of land under the 100-year flood level. River flood impact is defined as the average annual number of people exposed to reference period the 50-year flood, but because the indicator does not incorporate flood defences these people are not necessarily actually flooded. One of the coastal flood impact indicators is the average annual number of people estimated to be actually flooded in events that exceed flood defence standards, and this makes two different assumptions about how flood defence standards improve through time: the difference between the two characterises the effect of adaptation. The second coastal flood impact indicator is the number of people living below the 100-year flood level, ignoring defence levels.

2.3 Socio-economic scenarios

This assessment uses five Shared Socioeconomic Pathways (SSPs: O'Neill et al., 2017), which are based on five different narrative storylines for the future development of societies, economies and governance. They are plausible projections, rather than predictions. National population projections, by age, for each SSP are described by KC & Lutz (2017), and this analysis uses the population projections downscaled to the 0.5x0.5^{o} resolution by Jones & O'Neill (2016). The five SSPs differ in their assumptions about fertility and mortality, rates of urbanisation and international migration. Projections of national Gross Domestic Product are taken from Dellink et al. (2017) and downscaled to the 0.5x0.5^{o} resolution by assuming that each grid cell in a country has the same GDP per capita. GDP is used in the energy and coastal flood impact indicators. **Figure 2** shows the global total population and GDP through the 21st century under the five SSPs.

For the agricultural indicators, it is assumed that the areas of cropland (total and by crop: Supplementary Material) remain constant through the 21st century.

2.4 Calculation of damage functions

For the terrestrial indicators (Section 2.2), damage functions are constructed using climate scenarios from 23 atmosphere-ocean general circulation model patterns scaled, using ClimGEN (Osborn et al., 2016; 2018), to defined increases in global mean temperature and applied to a reference period

Accepted Manuscript

climatology. These scaled scenarios were constructed using pattern-scaling rather than time-slicing (James et al., 2017) in order to eliminate the effects of year-to-year and decade-to-decade variability on differences between scenarios at different levels of warming. 23 patterns for each climate variable (precipitation, precipitation variability, temperature, humidity and net radiation) were constructed from 23 CMIP5 climate models (listed in Supplementary Material), allowing the construction of 23 damage functions for each indicator, time period and socio-economic scenario. All 23 patterns are assumed to be equally plausible and independent. The changes in monthly climate were applied to the CRU TS4 0.5x0.5° 1981-2010 climatology (Harris et al., 2016) using the delta method in ClimGen (Osborn et al., 2016; 2018) to produce perturbed 30-year time series representing specific increases in global mean surface temperature. For precipitation, changes in monthly variability projected by climate models are also diagnosed and used within ClimGen to perturb the observed variability to represent the increased or decreased variability simulated by each climate model (see Osborn et al., 2016, for more details). This is important for those indicators that depend on climate variability as well as the mean climate. The climate scenarios do not incorporate the effects of naturally-forced multi-decadal variability on departures around the climate change trend, which would add to the range in projected impacts. The impacts models are applied at the 0.5x0.5° resolution and results averaged or aggregated to the regional and global scales.

The damage functions for the coastal indicators (Section 2.2) are constructed differently because impact in a given year is a function of sea-level rise rather than temperature increase, and the relationship between temperature increase in a given year and sea level rise depends on the rate of change in temperature. The coastal damage functions relating impact to global average sea level rise were therefore developed by running the Dynamic Interactive Vulnerability Assessment (DIVA) model (Vafeidis et al., 2008; Hinkel et al., 2014) with a range of sea-level rise scenarios describing change through the 21st century and plotting estimated impacts in a given year against sea-level rise in that year. The coastal indicators are calculated for coastal segments (which vary in length) and are aggregated to the regional and global levels.

2.5 Climate forcings and increases in temperature and sea level

The ScenarioMIP initiative (O'Neill et al., 2016) has defined a series of climate forcings for use by the climate modelling community to drive global climate model experiments, representing different trajectories of future greenhouse gas emissions. These include revisions to earlier Representative Concentration Pathways (RCP2.6, RCP4.5, RCP6.0 and RCP8.5) and three new pathways with radiative forcing at 2100 of 1.9, 3.4 and 7.0 W/m^2 (another overshoot pathway is not considered here). The new pathways are designed to fill gaps in the original range, and the revised pathways differ from the previous versions primarily through (i) the socio-economic scenarios used to define emissions of different greenhouse gases and aerosols, and (ii) the use of more up-to-date historical emissions and harmonisation between observations and scenarios. Impacts were calculated under all seven of the pathways (see Supplementary Material for full results), but the plots here focus for clarity on RCPs 2.6, 4.5 and 8.5. ScenarioMIP does not define a 'business-as-usual' emissions scenario, because 'business-as-usual' depends on socio-economic assumptions. The IPCC Fifth Assessment Report (Clarke et al., 2014) concluded that emissions scenarios with no specific assumptions about emissions reductions produced forcings between 6.0 and 8.5 W/m^2 by 2100. RCP8.5 is here used in the plots as an illustrative upper limit even though it may only arise under a relatively narrow set of circumstances (Riahi et al., 2017), for two primary reasons. First it continues to be widely used for climate model simulations, and second it is consistent with calls for the

Accepted Manuscript

presentation of the consequences of high-impact and 'worst-case' scenarios (King et al., 2015; Sutton, 2018).

Projections of the increase in global mean surface temperature for each of the RCP forcings (**Figure 3a**) were made using a probabilistic implementation of version 4.2 of the MAGICC energy balance model (Lowe et al., 2009; Lowe & Bernie, 2018). This probabilistic implementation samples across 1863 combinations of feasible values of equilibrium climate sensitivity (ECS), ocean diffusivity and carbon cycle feedback strength to produce 1863 projections of global mean temperature over time (each with a relative probability derived from the probability distributions of the ocean diffusivity and carbon cycle feedback strength parameters). The ECS values used are taken from the CMIP5 climate models assessed in the IPCC Fifth Assessment Report (Flato et al., 2013; Forster et al., 2013), and assumed to be equally plausible.

Impacts are estimated in each year (for a given socio-economic scenario) by combining the projected changes in temperature with the 23 equally-plausible damage functions (in practice percentiles from the distribution of temperature change in each year were used rather than the individual projections). The range in estimates of impact in each year under a specific climate and socio-economic pathway therefore represents uncertainty in (i) the increase in temperature in that year, which depends on equilibrium climate sensitivity, ocean diffusivity and carbon cycle feedback strength, and (ii) the spatial and seasonal distribution of change in relevant climate variables. The magnitude of impacts is characterised by the median, and the range is represented by the 10th and 90th percentiles of the distribution of impacts in each year (but should be interpreted as 'low' and 'high' rather than specific percentiles).

Sea level rise scenarios corresponding to the temperature forcings (**Figure 3b**) were constructed from the projected temperature changes using an empirical relationship between accumulated global temperature increase since 1985 and sea level rise relative to the 1986-2005 average level (Supplementary Material). This empirical relationship emulates the increase in sea level as presented in the IPCC AR5 (Church et al., 2013). The scenarios are globally uniform. For each emissions scenario, a central estimate of sea level rise is calculated from the time series of the median increase in temperature, and low and high sea level scenarios are calculated from the time series of the 10th and 90th percentile temperature changes. The range in estimated impacts in a year under a specific climate and socio-economic pathway just represents uncertainty in the sea-level rise by that year. The median sea level rise assumed here for RCP8.5 is similar to that projected by Kopp et al. (2014) and slightly lower than the estimate produced by Vousdoukas et al. (2018). The range here is between Kopp et al.'s (2014) 'likely' and 'very likely' ranges, but smaller than the range in Vousdoukas et al. (2018). Several projections of sea level rise made since AR5 have suggested larger high-end increases than presented in AR5 (Bamber et al., 2019), but there is considerable uncertainty over the effect of ice sheet melt. The high-end increases in sea level used in this study should therefore be regarded as conservative: coastal impacts could be considerably higher.

3 Results

3.1 Changes in hazard

Figure 4 shows the global-scale hazard indicators through the 21st century (Tables in Supplementary Material), under the seven RCP forcings. At the global aggregate scale, heatwave frequency increases (but at a different rate for the two heatwave definitions), drought frequency increases, flood frequency increases, the crop growth duration decreases (implying reduced yields), the

Accepted Manuscript

likelihood of hot spells damaging to crops increases, and cooling degree-days increase: all these are adverse consequences of climate change. Heating degree-days decrease, which is a potential benefit of climate change. Figure 4 shows the wide range in estimated future hazard, particularly for the indicators based on precipitation, but the range shown here does not suggest climate change could result in a reduction in hazard at the global scale for any of the indicators. The figure also demonstrates the large difference in future hazard occurrence between the different climate forcings, with the difference increasing after around 2040. Some of the hazard indicators level off at high levels of forcing. For the heatwave frequency indicator this is simply because everywhere experiences a heatwave every year. The runoff change indicator is – unlike the other indicators – just defined on the basis of whether or not a threshold is crossed, and this levels off with high levels of forcing as fewer and fewer additional areas exceed the threshold

The variation in aggregated hazard indicator by continent in 2100 is shown in **Figure 5** (variation across regions is shown in Supplementary Material, which also includes plots showing each hazard indicator by region). The height of the individual bars represents scientific uncertainty (Section 3.2). For the indicators dependent on temperature, the bars typically do not overlap, indicating that uncertainty in the rate of forcing is large relative to the scientific uncertainty; for the precipitation-based indicators, the bars overlap indicating that scientific uncertainty is large relative to emissions uncertainty.

There is greater variability between continents with the major heatwave indicator than for the more moderate heatwave indicator (because this saturates at 100% with high emissions), and even more variability with the heatwave duration indicator. This indicator shows the greatest increase in heatwave duration in Africa, South America, Asia (especially south east Asia) and Australasia.

Hydrological drought frequency increases in each continent, but with low climate forcing there could be very little change in Asia and North America. With the highest forcing, the greatest increase in hydrological drought frequency is in Europe, South America (especially central America and Brazil), the Middle East and North Africa, and Australasia, but with wide uncertainty between climate model patterns. Agricultural drought frequency increases in every continent under all scenarios, but the difference between regions is less marked.

The greatest increase in river flood frequency is in Asia (especially south and south east Asia) and Africa, with relatively small change with low forcings in Europe and North America (and frequency could decrease).

Europe and North America see the greatest reductions in crop growth duration – and therefore potentially yield - for all crops (to the least extent for winter wheat). Maize and winter wheat hot spell frequencies increase most in Europe and North America (especially the USA), but the frequency of hot spells for soybean, spring wheat and rice increases most in Africa and Asia: Europe and North America are relatively unaffected.

The absolute changes in cooling degree days are in Asia and Africa, but the greatest relative increases are in Europe and North America. The greatest absolute decreases in heating degree days are in Asia, Europe and North America, but the greatest relative decreases are in Africa.

3.2 Sources of uncertainty

Accepted Manuscript

The plots in Figures 4 and 5 show the median estimate, plus the range between 'low' and 'high' hazard indicator for each climate forcing. For a given level of climate forcing, the range for an indicator represents uncertainty in (i) the change in global mean temperature (a function of equilibrium climate sensitivity (ECS), ocean diffusivity and carbon cycle feedback) and (ii) the spatial pattern of change in temperature and precipitation. **Figure 6** shows the relative importance of each of these sources of uncertainty for each hazard indicator (except for the coastal indicator) under the highest level of forcing (RCP8.5) and at the global scale. The maximum uncertainty for each indicator is shown when the uncertainty contributions sum to 100% in Figure 6. The uncertainty range of most indicators increases over time and reaches its maximum in 2100. The uncertainty ranges of the two heatwave and the rice heat stress indicators peak earlier in the century and then decline because at large changes in climate everywhere is impacted under all parameter combinations so uncertainty reduces. The plots show that uncertainty in the equilibrium climate sensitivity is much more important than uncertainty in the strength of the carbon cycle feedback or ocean diffusivity, but that for the indicators determined by precipitation change the scientific uncertainty is dominated by the uncertainty in the spatial distribution of change in rainfall as represented by different climate models. The selection of models used to estimate impacts therefore has a greater effect on the estimated uncertainty range.

3.3 Socio-economic impact

Figure 7 shows the global socio-economic impact of changes in hazard indicators in 2050 and 2100 (Tables in Supplementary Material). The figure focuses for clarity on three climate forcings (RCP2.6, RCP4.5 and RCP8.5) and for the population indicators shows impact under all five socio-economic scenarios (the agricultural indicators are all expressed in terms of area of cropland affected, which is assumed to remain constant over time). In 2050 there is relatively little difference in impact between the three levels of forcing, but by 2100 the difference is much greater. Again, the height of the individual bars represents scientific uncertainty.

Even by 2050, however, there is a difference in impact between the five socio-economic scenarios, and this difference increases further by 2100. Scenario SSP3 has the highest total population, so has the highest impact on heatwaves, floods, droughts and the population living in watersheds which cease to be water-stressed. More people live in watersheds that become water-stressed under SSP2 than the other scenarios, and this is because of the geographical distribution of the increase in population.

By 2050, the range in impact across the climate forcings is greater than the range across the socio-economic scenarios for major heatwaves, heatwave duration, and the population exposed to river flooding (Supplementary Material). The range across socio-economic scenarios is greater than the range across the climate forcings for heatwave impacts (possibly here because of the saturation at high levels of forcing noted above), energy demand, exposure to water resources scarcity and coastal flood exposure. By 2100, the range across climate forcings is greater than the range across socio-economic scenarios only for major heatwaves and heatwave duration impacts, and the greater range across socio-economic scenarios is more apparent than in 2050.

The socio-economic impacts of climate change are – at the global scale - adverse for most, but not all the socio-economic indicators. Residential heating energy requirements decline with higher temperatures, and by 2050 the global total residential heating and cooling demands are lower than they would be without climate change under all the climate forcings and socio-economic scenarios. By 2100, however, the increases in cooling energy demand outstrip the reductions in heating

Accepted Manuscript

demand in three of the socio-economic scenarios (SSP1, SSP2 and SSP5), so total demands are increased. At the global scale, more people live in watersheds that ceased to be water-stressed than live in watersheds that become water-stressed, particularly under the high population SSP3 and increasingly through the 21st century. This is different to the distribution of change in runoff (Figure 4), because the areas with an increase in runoff are more populous than areas with a decrease. Note that the drought indicator represents a different dimension to water resources stress, as droughts can occur in regions that are not water-stressed.

The variation in impact between continents and regions can be expressed in two ways. Expressing impacts in *absolute* terms - people, area of cropland and energy use – gives an indication of the absolute magnitude of impact in a region and the contribution of a region to the global total impact. Expressing impacts in *relative* terms – as a proportion of population or cropland, for example – gives an indication of the relative significance of an impact in a region. A third approach would be to show impacts as a proportional change from a reference period. Each is policy relevant. The distribution of *absolute* socio-economic impact in 2100 across continents by indicator is shown in **Figure 8** (just for SSP2 for the population indicators: the variation between continents is broadly similar with the other SSPs. Supplementary Material also shows distribution by region and allows the calculation of impacts in relative terms). The plots show the indicators in 2100 with the value for 2100 assuming no climate change, and give an indication of the effect of climate change relative to the reference climate. The river flooding and cropland indicators also show the total floodplain population and cropland area, and therefore give an indication of the relative importance of the impact in each region.

In absolute terms, the greatest impact of climate change on people exposed to heatwaves is in Asia (especially south and east), followed by Africa. The greatest number of people exposed to an increase in water scarcity are in (west) Africa, and most people exposed to river and coastal flooding are in Asia, especially south Asia. Asia also sees the largest number of people living in watersheds that cease to be defined as water-scarce by 2100 (mostly in south Asia). Africa and Asia have the greatest number of people exposed to hydrological drought. The greatest absolute cooling energy requirements by 2100 are in (south) Asia and (west) Africa, whilst heating energy requirements are concentrated in (east) Asia, Europe and North America but are projected to decrease sharply with greater climate warming. The greatest absolute areas of cropland exposed to drought are in Asia and Europe. Large areas of maize and winter wheat across all continents see a reduction in crop growth duration of at least 10 days, but extensive areas with reductions in duration for soybean and spring wheat are concentrated in North America and Asia. Large proportions of the rice-growing areas in Asia see reductions in duration of at least 10 days. The greatest proportion of maize-growing areas affected by damaging hot spells is in North America (USA), and an increasing frequency of damaging hot spells for soybean is most widespread in south Asia. Winter wheat growing areas are more affected by damaging hot spells than spring wheat areas (except for south Asia). The rice growing areas in west Africa, south and south east Asia are most affected by hot spells: east Asia is little affected.

3.4 A summary: multiple indicators across a region

The previous figures have shown each indicator separately, across each continent (Figure 5 and Figure 8) and region (Supplementary Material). **Figures 9** and **10** show all the hazard and impact indicators together for each continent (by region in Supplementary Material). This form of presentation allows an evaluation of how a region is affected by change in each indicator.

Accepted Manuscript

4 Discussion

There are, of course, several caveats with this study. The temperature scenarios incorporate current best estimates of uncertainty in climate sensitivity, carbon cycle feedbacks and ocean diffusivity, and these estimates change as more evidence becomes available. The climate scenarios were constructed using pattern-scaling and the delta method and making specific assumptions about disaggregating monthly climate data to the daily scale: other methods are available. It was assumed that each of the CMIP5 climate model patterns of change was equally plausible and independent, and can be matched with any increase in global mean temperature. A different ensemble of model runs – for example using higher resolution models – could give a different spread of results. The sea level rise scenarios use an empirical relationship between accumulated temperature and sea level rise tuned to results from the IPCC AR5, and assume that sea level rise is globally-uniform. The study uses a series of indicators that represent the consequences of climate change for future hazards and socio-economic impacts, but do not describe actual impacts: these will depend on current and future adaptation decisions. Different global-scale studies have used different indicators of similar dimensions of hazard and impact, hindering comparisons of results between the different studies. The impacts as defined by the different socio-economic indicators are not directly comparable, because they are expressed – for practical reasons – in different units (numbers of people, numbers of people per year etc). Even where the units are the same, it is not necessarily straightforward to compare the magnitude of impacts. Is one person exposed to flooding equal to one person exposed to drought equal to one person exposed to heatwave, for example?

Nevertheless, the study has determined in a consistent way multiple indicators of hazards, resource base and impacts across regions, sectors, climate forcings and socio-economic scenarios. The Supplementary Material includes information presented in different formats. The study provides the foundation for more nuanced assessments of implications for the distribution of impact across regions and for the development of narrative storylines describing implications of climate change for, for example, resilience, supply chains and security. The study shows the wide uncertainty range in estimated changes in hazard and impact. For the water-related indicators, this is primarily due to uncertainty in the projected change in precipitation across space. This wide range, together with the observation that the estimated shape of the distribution of potential consequences in a year is not necessarily uni-modal, demonstrates that the selection of climate models for an assessment can have a major effect on the estimated range – and potentially even direction – in change.

5 Conclusions

This paper has used a consistent set of climate and socio-economic scenarios to present changes in a wide range of indicators of hazard and socio-economic impact at regional and global scales through the 21st century. It incorporates uncertainty in future emissions and socio-economic scenarios, alongside the effects of scientific uncertainty. It provides a quantitative foundation (in the paper and in Supplementary Material) both for risk assessments based on explicit categories of impact and for more nuanced qualitative assessments of the consequences of climate change using narrative characterisations of changes in key drivers such as governance and policy.

At the global scale, all the aggregated consequences of climate change considered here are adverse, with the exception of requirements for heating energy. However, the uncertainty range is large, primarily due to uncertainty in the projected regional change in precipitation, and the 'high end' consequences under each of the climate forcings considered can be much greater than the median estimate. For example, by 2100 and under RCP8.5 the median estimate of the global average

Accepted Manuscript

proportion of time in hydrological drought is 27%, but the high-end estimate is 36%; the median estimate of the global average return period of the current 50-year flood is 14 years (7% likelihood), but the high-end estimate is 9 years (11% likelihood).

The uncertainty range for a few of the precipitation-related indicators (floods and droughts) in some regions includes both adverse and beneficial consequences, reflecting regional variability in the direction of change in rainfall. There is a clear difference in hazard and impact under the different levels of climate forcing, with the difference varying across the indicators. Even under the lowest forcing there are substantial changes in hazard and impact by 2100. The assumed future socio-economic scenario has a very large effect on the estimated impacts of a given level of forcing, and for most socio-economic indicators the range in impact is greater across the socio-economic scenarios than the climate forcings. This highlights the strong dependence of future impacts of climate change on socio-economic change.

Accepted Manuscript

Acknowledgements

This work develops from research funded through the UK AVOID2 programme (UK Department for Business, Enterprise and Industrial Strategy grant 1104872). TJO acknowledges the support provided by the EU HELIX project (grant number 603864) for incorporating the CMIP5 climate model patterns into ClimGEN. We acknowledge the World Climate Research Programme's Working Group on Coupled Modelling, which is responsible for CMIP, and we thank the climate modeling groups (listed in Supplementary Material) for producing and making available their model output. For CMIP the U.S. Department of Energy's Program for Climate Model Diagnosis and Intercomparison provides coordinating support and led development of software infrastructure in partnership with the Global Organization for Earth System Science Portals.

Data Availability Statement

Any data that support the findings of this study are included within the article and in online Supplementary Material.

Accepted Manuscript

References

Alfieri, L. et al. (2017) Global projections of river flood risk in a warmer world. *Earths Future* 5(2): 171-182.

Arnell, N.W. & Gosling, S.N. (2016) The impacts of climate change on river flood risk at the global scale. *Climatic Change* 134, 387-401.

Arnell, N.W. & Lloyd-Hughes, B. (2014) The global-scale impacts of climate change on water resources and flooding under new climate and socio-economic scenarios. *Climatic Change* 122: 127-140

Arnell, N.W. et al. (2013) A global assessment of the effects of climate policy on the impacts of climate change. *Nature Climate Change* 3, 512-519.

Arnell, N.W. et al. (2016a) Global-scale climate impact functions: the relationship between climate forcing and impact. *Climatic Change* 134, 475-487

Arnell, N.W. et al. (2016b) The impacts of climate change across the globe: a multi-sectoral assessment. *Climatic Change* 134, 457-474.

Arnell, N.W. et al. (2019) Global and regional impacts of climate change at different levels of global temperature increase *Climatic Change* doi 10.1007/s10584-019-02464-z

Bamber, J.L. et al. (2019) Ice sheet contributions to future sea-level rise from structured expert judgment. *Proceedings, National Academy of Sciences* 116, 11195-11200.

Betts, R. A. et al. (2018) Changes in climate extremes, fresh water availability and vulnerability to food insecurity projected at 1.5 degrees C and 2 degrees C global warming with a higher-resolution global climate model. *Philosophical Transactions of the Royal Society a-Mathematical Physical and Engineering Sciences* 376(2119).

Byers, E. et al. (2018) Global exposure and vulnerability to multi-sector development and climate change hotspots. *Environmental Research Letters* 13(5).

Challinor, A.J. et al. (2016) Current warming will reduce yields unless maize breeding and seed systems adapt immediately. *Nature Climate Change* 6, 954-958.

Church, J.A. et al. (2013) Sea level change. In *Climate Change 2013: The Physical Science Basis* (eds. Stocker, T.F. et al. (eds.) (Cambridge University Press).

Clarke L. et al. (2014) Assessing Transformation Pathways. In: *Climate Change 2014: Mitigation of Climate Change. Contribution of Working Group III to the Fifth Assessment Report of the Intergovernmental Panel on Climate Change* [Edenhofer, O. et a. (eds.)]. Cambridge University Press, Cambridge, United Kingdom and New York, NY, USA

Dellink, R. et al. (2017) Long-term economic growth projections in the Shared Socioeconomic Pathways. *Global Environmental Change* 42, 200-214.

Dosio, A. et al. (2018) Extreme heat waves under 1.5°C and 2°C global warming. *Environmental Research Letters* 13 054006

Flato, G. (2013) Evaluation of Climate Models. In: *Climate Change 2013: The Physical Science Basis. Contribution of Working Group I to the Fifth Assessment Report of the Intergovernmental Panel on Climate Change* [Stocker, T.F. et al. (eds.)]. Cambridge University Press, Cambridge, United Kingdom and New York, NY, USA.

Forster, P.M. et al. (2013) Evaluating adjusted forcing and model spread for historical and future scenarios in the CMIP5 generation of climate models. *Journal of Geophysical Research Atmospheres* 118, 1139-1150. doi:10.1002/jgrd.50174

Gosling, S.N. & Arnell, N.W. (2016) A global assessment of the impact of climate change on water scarcity. *Climatic Change* 134, 371-385.

Gourdji, S.M., Sibley, A.M. & Lobell, D. B. (2013) Global crop exposure to critical high temperatures in the reproductive period: historic trends and future projections. *Environmental Research Letters* 8: 24041

Harrington, L. J. et al. (2018) How uneven are changes to impact-relevant climate hazards in a 1.5 degrees C world and beyond? *Geophysical Research Letters* 45(13): 6672-6680.

Harris, I. et al. (2014) Updated high-resolution grids of monthly climatic observations – the CRU TS3.10 dataset. *Int. J. Climatol*. 34, 623-642.

Accepted Manuscript

Hinkel, J. et al. (2014) Coastal flood damage and adaptation costs under 21st century sea-level rise. *Proc. Nat. Acad, Sci*. 111 (9), 3292-3297.

Hsaing, S. et al. (2017) Estimating economic damage from climate change in the United States. *Science* 356, 1362-1369.

James, R. et al. (2017) Characterizing half-a-degree difference: a review of methods for identifying regional climate responses to global warming. *WIREs Climate Change* 8:e457. doi:10.1002/wcc.457

Jones, B. & O'Neill, B.C. (2016) Spatially explicit global population scenarios consistent with the Shared Socioeconomic Pathways. *Environmental Research Letters* 11(8) 10.1088/1748-9326

KC, S. & Lutz, W. (2017) The human core of the shared socio-economic pathways: population scenarios by age, sex and level of education for all countries to 2100. *Global Environmental Change* 42: 181-192.

King, D., Schrag, D., Dadi, Z et al. (2015) *Climate Change: A Risk Assessment.* Centre for Science and Policy, University of Cambridge

Kopp, R.E. et al. (2014) Probabilistic 21st and 22nd century sea-level projections at a global network of tide-gauge sites. *Earths Future* 2, 383–406

Lehner, F. et al. (2018) Future risk of record-breaking summer temperatures and its mitigation. *Climatic Change* 146: 363-375.

Lowe, J.A. et al. (2009) How difficult is it to recover from dangerous levels of global warming? *Environ. Res. Lett*. 4, 014012.

Naumann, G. et al. (2018) Global Changes in Drought Conditions Under Different Levels of Warming. *Geophysical Research Letters* 45(7): 3285-3296.

O'Neill, B.C. et al. (2016) The Scenario Model Intercomparison Project (ScenarioMIP) for CMIP6. *Geosci. Model Dev*., 9, 3461-3482.

O'Neill, B.C. et al. (2017) The roads ahead: narratives for shared socioeconomic pathways describing world futures in the 21st century. *Global Environmental Change* 42: 169-180.

O'Neill, B.C. et al. (2018) The Benefits of Reduced Anthropogenic Climate change (BRACE): a synthesis. *Climatic Change* 146: 287-301.

Osborn, T.J. et al. (2016) Pattern-scaling using ClimGen: monthly-resolution future climate scenarios including changes in the variability of precipitation. *Climatic Change* 134, 353-369.

Osborn T.J. et al. (2018) Performance of pattern-scaled climate projections under high-end warming, part I: surface air temperature over land. *Journal of Climate* **31**, 5667-5680

Riahi, K. et al. (2017) The Shared Socioeconomic Pathways and their energy, land use, and greenhouse gas emissions implications: an overview. *Global Environmental Change* 42, 153-168.

Ruane, A. C., M. M. Phillips and C. Rosenzweig (2018) Climate shifts within major agricultural seasons for+1.5 and+2.0 degrees C worlds: HAPPI projections and AgMIP modeling scenarios. *Agricultural and Forest Meteorology* 259: 329-344.

Schleussner, C. F. et al. (2016) Differential climate impacts for policy-relevant limits to global warming: the case of 1.5 degrees C and 2 degrees C. *Earth System Dynamics* 7(2): 327-351.

Seneviratne, S. et al. (2016) Allowable CO2 emissions based on regional and impact-related climate targets. *Nature* 529, 477-483

Schleussner, C. F. et al. (2018) Crop productivity changes in 1.5 degrees C and 2 degrees C worlds under climate sensitivity uncertainty. *Environmental Research Letters* 13(6).

Shukla, S., and A. W. Wood (2008) Use of a standardized runoff index for characterizing hydrologic drought, *Geophys. Res. Lett*., 35 10.1029/2007GL032487

Smirnov, O. et al. (2016) The relative importance of climate change and population growth for exposure to future extreme droughts. *Climatic Change* 138(1-2): 41-53.

Sutton, R. (2018) ESD Ideas: a simple proposal to improve the contribution of IPCC WG1 to the assessment and communication of climate change risks. *Earth System Dynamics* 9, 1155-1158.

Tebaldi, C. & Lobell, D. (2018) Estimated impacts of emission reductions on wheat and maize crops.

Accepted Manuscript

Climatic Change 146: 533-545.

Tebaldi, C. & Wehner, M.F. (2018) Benefits of mitigation for future heat extremes under RCP4.5 compared to RCP8.5. *Climatic Change* 146: 349-361.

UNEP (2018) *Emissions Gap Report 2018*. United Nations Environment Programme

Vafeidis, A.T. et al. (2008) A new global coastal database for impact and vulnerability analysis to sea-level rise. *Journal of Coastal Research* 24, 917–924 (2008).

van Vuuren, D.P. et al. (2014) A new scenario framework for climate change research: scenario matrix architecture. *Climatic Change* 122, 373–386.

Vicente-Serrano, S.M. et al. (2010) A multi-scalar drought index sensitive to global warming: the standardised precipitation evapotranspiration index – SPEI. *J. Climate* 23, 1696-1711.

Vousdoukas, M.I. et al. (2018) Global probabilistic projections of extreme sea levels show intensification of coastal flood hazard. *Nature Communications* 10.1038/s41467-018-04692-w

Winsemius, H. C. et al. (2016) Global drivers of future river flood risk. *Nature Climate Change* 6(4): 381-385.

Accepted Manuscript

Table 1: Hazard, resource and impact indicators

Hazard / resource indicator		Impact indicator	Additional information
Heat extremes			
Heatwave frequency: annual % chance of experiencing at least one at a given location(p)	A heatwave is a period of at least two days with daily maximum temperature greater than the 98th percentile of warm season temperatures, at a given location	Average annual population exposed to at least one heatwave: millions/year	
Major heatwave frequency: annual % chance of experiencing at least one at a given location(p)	A heatwave is a period of at least four days with daily maximum temperature greater than the 99th percentile of warm season temperatures, at a given location	Average annual population exposed to at least one major heatwave: millions/year	
Heatwave duration: average annual number of heatwave-days at given location(p)	A heatwave is a period of at least two days with daily maximum temperature greater than the 98th percentile of warm season temperatures, at a given location	Average annual population exposed to heatwaves: million people-days/year	
Water			
Area with increase or decrease in average annual runoff: % of area	A significant increase or decrease in runoff is more than twice the standard deviation of 30-year mean runoff.	Population living in watersheds that become water-stressed, or cease to be water-stressed: millions	A water-stressed watershed has average annual runoff less than 500 m^3/capita/year
Duration of hydrological drought: % of time in drought at a given location(p)	Hydrological drought occurs when the 12-month accumulated Standardised Runoff Index (SRI: Shukla & Wood, 2008) is less than -1.5	Average annual population exposed to drought: millions/year	A drought is a period of at least six months with 12-month SRI less than -1.5
Floods			
Frequency of reference period 50-year (2%) river flood: annual % likelihood at a given location(p)	Flood frequency is estimated by fitting a Generalised Extreme Value (GEV) distribution to simulated river flows (Arnell & Gosling, 2016)	Average annual population exposed to river flooding: millions/year	Population living in identified river floodplains multiplied by the average annual likelihood of experiencing a flood greater than the reference 50-year flood
Area of coastal land below the 100-year coastal flood level: thousand km^2	100-year return period coastal flood level estimated using the DIVA model (Vafeidis, et al., 2008)	Coastal population living below the 100-year flood level: millions	100-year return period coastal flood level estimated using the DIVA model, ignoring coastal flood defences
		Average annual number of people flooded in coastal floods: millions/year	Flood levels estimated using DIVA, with two assumptions about changing levels of coastal defences
Agriculture			
Duration of agricultural drought: % of time in drought at a given location(c)	Agricultural drought occurs when the 6-month accumulated Standardised Precipitation Evaporation Index (SPEI: Vicente-Serrano et al., 2010) is less than -1.5	Average annual area of cropland exposed to drought: thousand km^2/year	A drought is a period of at least three months with 6-month SPEI less than -1.5
Change in average annual crop growth duration: days at a given location(c)	Crop growth duration is based on the time to accumulate reference period thermal degree-days, with thresholds	Average annual area of cropland with reduction in average crop growth	Cropland area differs between the five crops

Accepted Manuscript

	varying between five crops: maize, winter wheat, spring wheat, rice and soybean	duration of at least 10 days: thousand km^2/year	
Frequency of damaging hot spells during crop reproductive season: annual % chance at a given location[(c)]	The temperature threshold and timing of reproductive season varies between the five crops: maize, winter wheat, spring wheat, rice and soybean	Average annual area of cropland experiencing a damaging hot spell: thousand km^2/year	Cropland area differs between the five crops
Energy			
Cooling degree days: days/year [(p)]	Average annual cooling-degree days relative to 18^{o}C, in a given location.	Cooling energy demands: PJ	Average annual residential cooling energy demands (Isaac & van Vuuren, 2008)
Heating degree days: days/year[(p)]	Average annual heating-degree days relative to 18^{o}C, in a given location.	Heating energy demands: PJ	Average annual residential heating energy demands
		Cooling and heating energy demands: PJ	Sum of residential cooling and heating demands

See Supplementary Material for more details and references

[(p)] regional averages weighted by grid cell area, omitting grid cells with fewer than 1000 people in 2010.

[(c)] regional averages weighted by cropland area.

Accepted Manuscript

Figures

Figure 1: Illustration of the methodology. Damage functions showing impact in a given year against increase in global mean temperature (1a) are combined with the distribution of the increase in temperature in that year (1b) to produce a distribution of impacts in that year (1c). The individual lines in 1a are the damage functions constructed from different climate model patterns. The dotted vertical lines in 1c show the 10th and 90th percentiles, and the solid vertical line shows the median.

Figure 2: Global total population and GDP under the five Shared Socioeconomic Pathways (SSPs).

Figure 3: Increase in global mean surface temperature and global mean sea level, under the seven forcing scenarios. For temperature, the solid line represents the median estimate and the shaded area the 10th to 90th percentiles. For sea level, the solid line represents a central estimate and the shaded area the range between a 'low' and 'high' estimate.

Figure 4: Global hazard indicators to 2100, under RCP2.6, RCP4.5 and RCP8.5. The bars on the right show impacts in 2100 under seven RCPs. The dotted line shows the value of the indicator under the 1981-2010 climate (1986-2005 sea level). The solid line represents the median and the shaded area the range between the 10th and 90th percentiles ("low" and "high" for the coastal indicator).

Figure 5: Hazard indicators across continents in 2100: RCP2.6, RCP4.5 and RCP8.5. The solid black lines show indicators under the 1981-2010 climate (1986-2005 sea level). The solid line represents the median and the shaded area the range between the 10th and 90th percentiles ("low" and "high" for the coastal indicator).

Figure 6: Relative importance of different sources of scientific uncertainty in the projected hazard indicators: RCP8.5, global scale. The plots show the contribution of uncertainties in equilibrium climate sensitivity (ECS), carbon cycle feedback, ocean diffusivity and climate model pattern to the total uncertainty in the projected impacts in each year. Uncertainty is characterised by the average variance in the distribution of estimated impacts in a year across each source of uncertainty. The contributions of each source are expressed as a % of the maximum total sum of the variances across all years: this is usually 2100.

Figure 7a: Global impact indicators in 2050: RCP2.6, RCP4.5 and RCP8.5. The solid line represents the median and the shaded area the range between the 10th and 90th percentiles ("low" and "high" for the coastal indicator). The horizontal grey and black lines are impacts in 2010 and 2050 respectively with the 1981-2010 climate (1986-2010 sea level). The five bars for each RCP represent the five Shared Socio-economic Pathways. The vertical axis limits for the cropland indicators are determined by total cropland area.

Figure 7b: Global impact indicators in 2100

Figure 8: Impact indicators for each continent in 2100: RCP2.6, RCP4.5 and RCP8.5. SSP2 socio-economic scenario for the population indicators. The solid line represents the median and the shaded area the range between the 10th and 90th percentiles ("low" and "high" for the coastal indicator). For the cropland indicators, the green lines show the total regional cropland area, and for the river flood indicator the green line shows the total regional river floodplain population.

Figure 9: Overview of continental hazard indicators: 2100: RCP2.6, RCP4.5 and RCP8.5. The solid line represents the median and the shaded area the range between the 10th and 90th

Accepted Manuscript

percentiles ("low" and "high" for the coastal indicator). The axis limits for each indicator are shown at the top of each column. The axis limits vary across continents.

Figure 10: Overview of continental impact indicators: 2100: RCP2.6, RCP4.5 and RCP8.5. SSP2 socio-economic scenario for the population indicators. The solid line represents the median and the shaded area the range between the 10th and 90th percentiles ("low" and "high" for the coastal indicator). The axis limits for each indicator are shown at the top of each column. The axis limits vary across continents. For the cropland indicators the limits are the total regional continental cropland area, and for the river flood indicator the limits are the total regional river floodplain population.

Accepted Manuscript

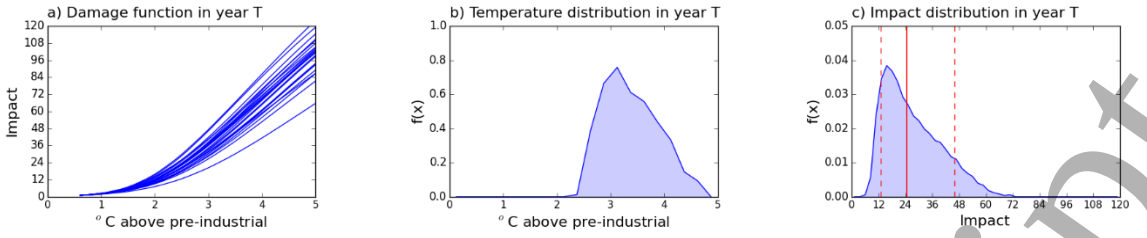

Figure 1: Illustration of the methodology. Damage functions showing impact in a given year against increase in global mean temperature (1a) are combined with the distribution of the increase in temperature in that year (1b) to produce a distribution of impacts in that year (1c). The individual lines in 1a are the damage functions constructed from different climate model patterns. The dotted vertical lines in 1c show the 10th and 90th percentiles, and the solid vertical line shows the median.

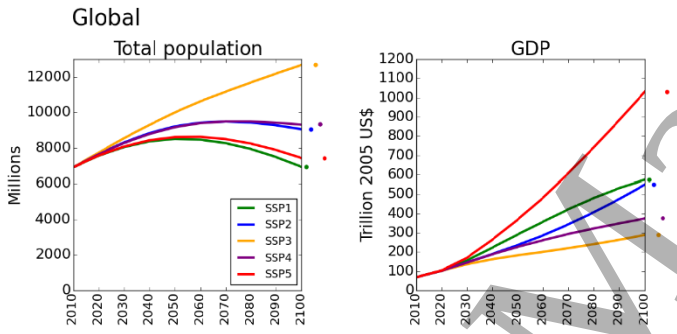

Figure 2: Global total population and GDP under the five Shared Socioeconomic Pathways (SSPs).

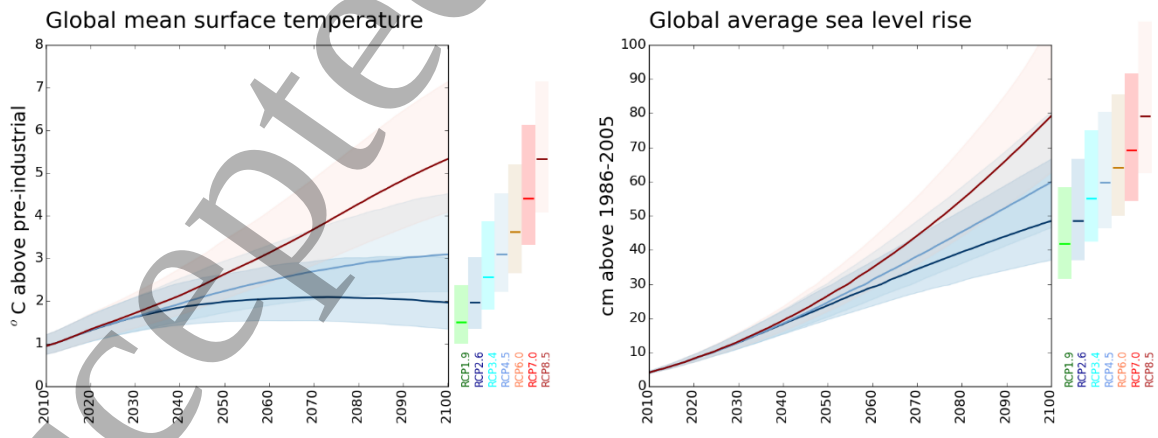

Figure 3: Increase in global mean surface temperature and global mean sea level, under the seven forcing scenarios. For temperature, the solid line represents the median estimate and the

Accepted Manuscript

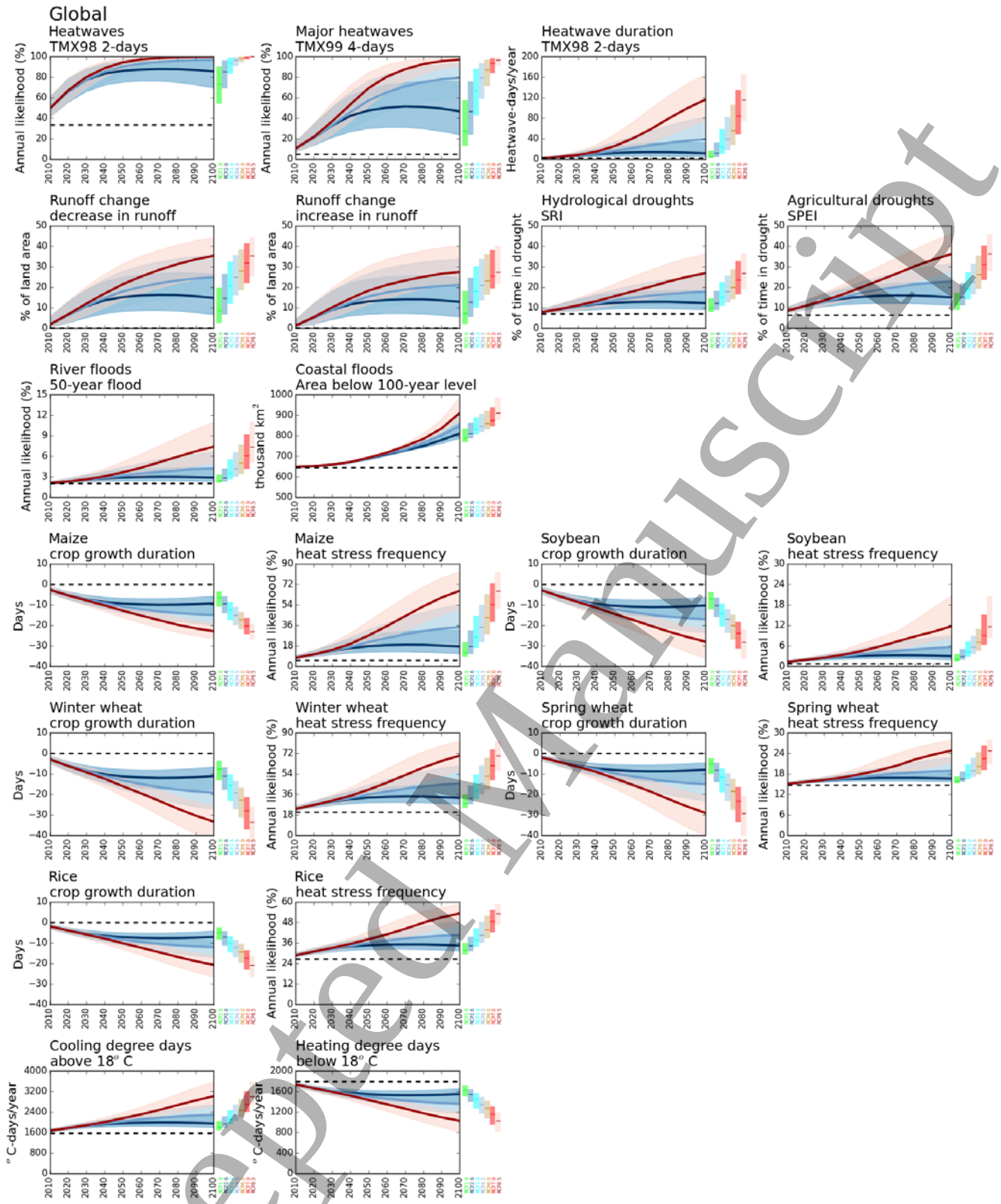

Figure 4: Global hazard indicators to 2100, under RCP2.6, RCP4.5 and RCP8.5. The bars on the right show impacts in 2100 under seven RCPs. The dotted line shows the value of the indicator under the 1981-2010 climate (1986-2005 sea level). The solid line represents the median and the shaded area the range between the 10th and 90th percentiles ("low" and "high" for the coastal indicator).

Accepted Manuscript

Figure 5: Hazard indicators across continents in 2100: RCP2.6, RCP4.5 and RCP8.5. The solid black lines show indicators under the 1981-2010 climate (1986-2005 sea level). The solid line represents the median and the shaded area the range between the 10th and 90th percentiles ("low" and "high" for the coastal indicator).

Accepted Manuscript

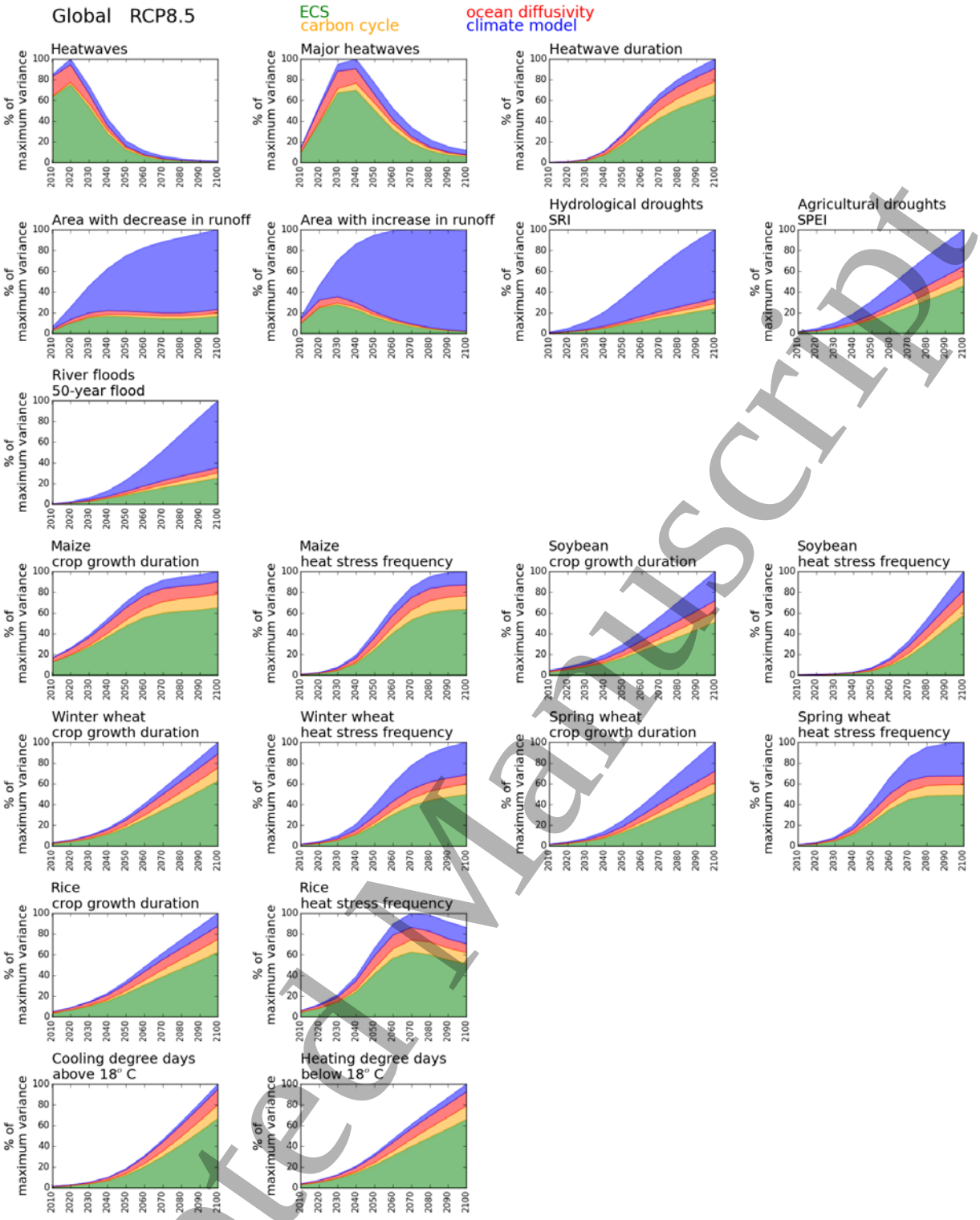

Figure 6: Relative importance of different sources of scientific uncertainty in the projected hazard indicators: RCP8.5, global scale. The plots show the contribution of uncertainties in equilibrium climate sensitivity (ECS), carbon cycle feedback, ocean diffusivity and climate model pattern to the total uncertainty in the projected impacts in each year. Uncertainty is characterised by the average variance in the distribution of estimated impacts in a year across each source of uncertainty. The contributions of each source are expressed as a % of the maximum total sum of the variances across all years: this is usually 2100.

Accepted Manuscript

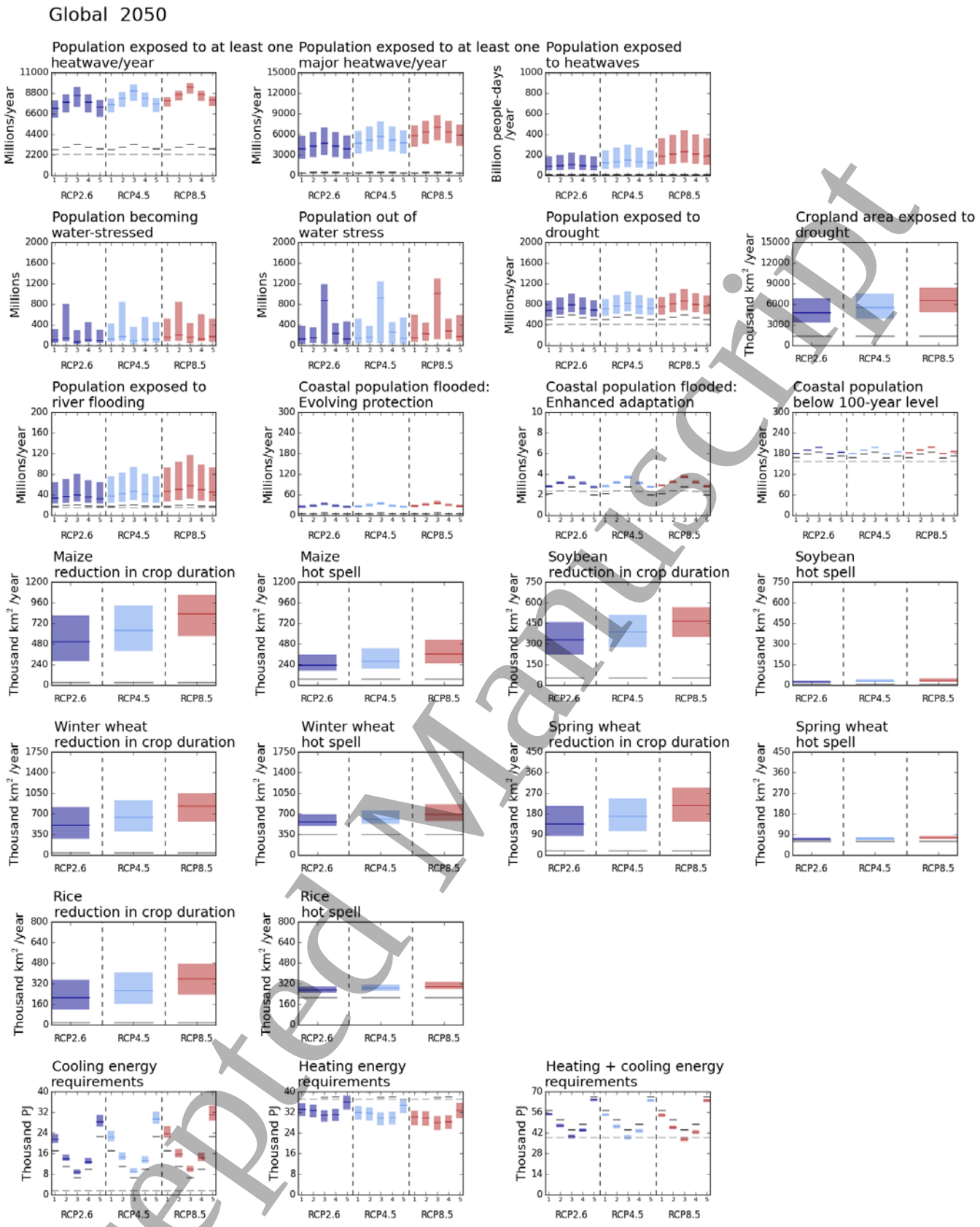

Figure 7a: Global impact indicators in 2050: RCP2.6, RCP4.5 and RCP8.5. The solid line represents the median and the shaded area the range between the 10th and 90th percentiles ("low" and "high" for the coastal indicator). The horizontal grey and black lines are impacts in 2010 and 2050 respectively with the 1981-2010 climate (1986-2010 sea level). The five bars for each RCP represent the five Shared Socio-economic Pathways. The vertical axis limits for the cropland indicators are determined by total cropland area.

Accepted Manuscript

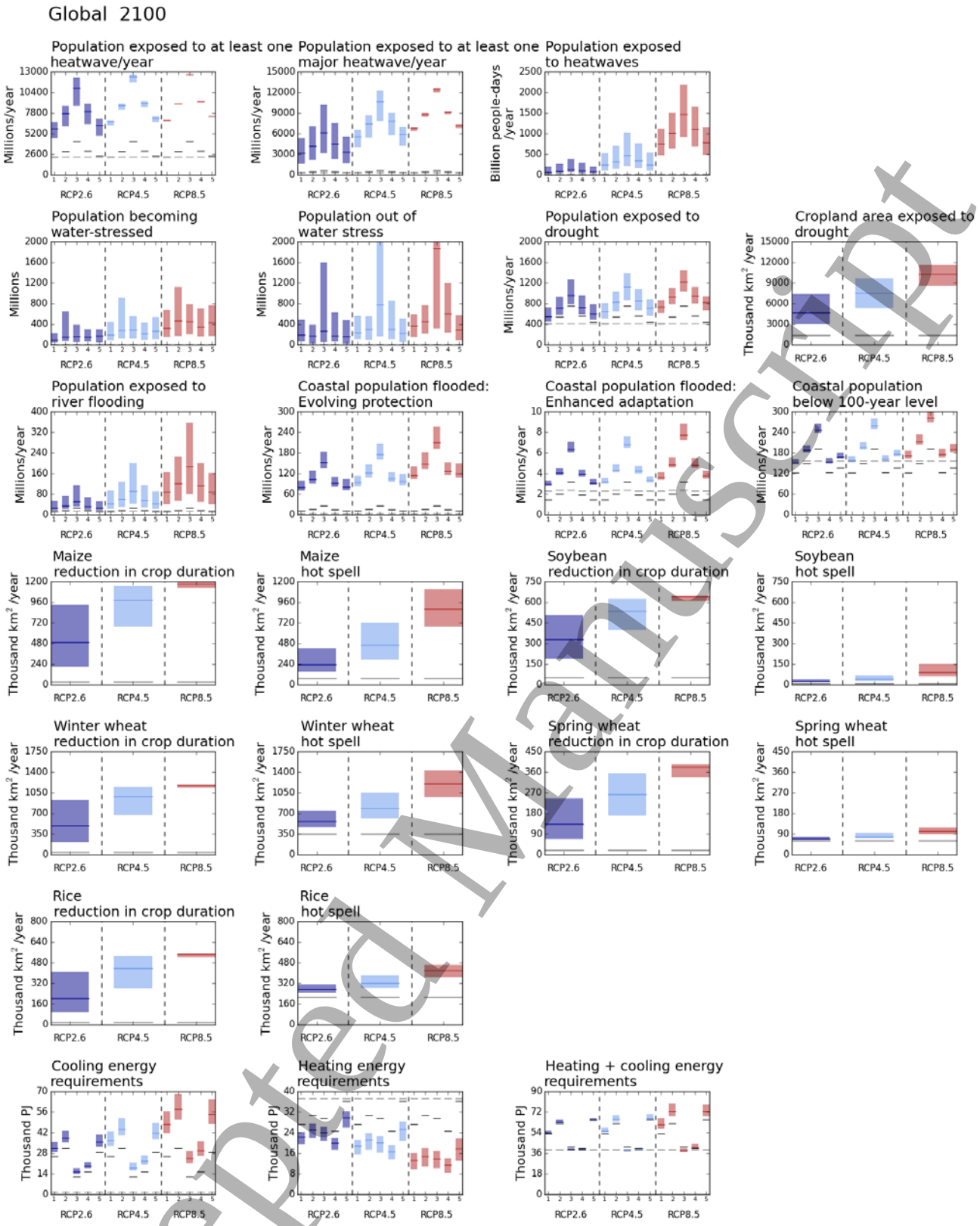

Figure 7b: Global impact indicators in 2100

Accepted Manuscript

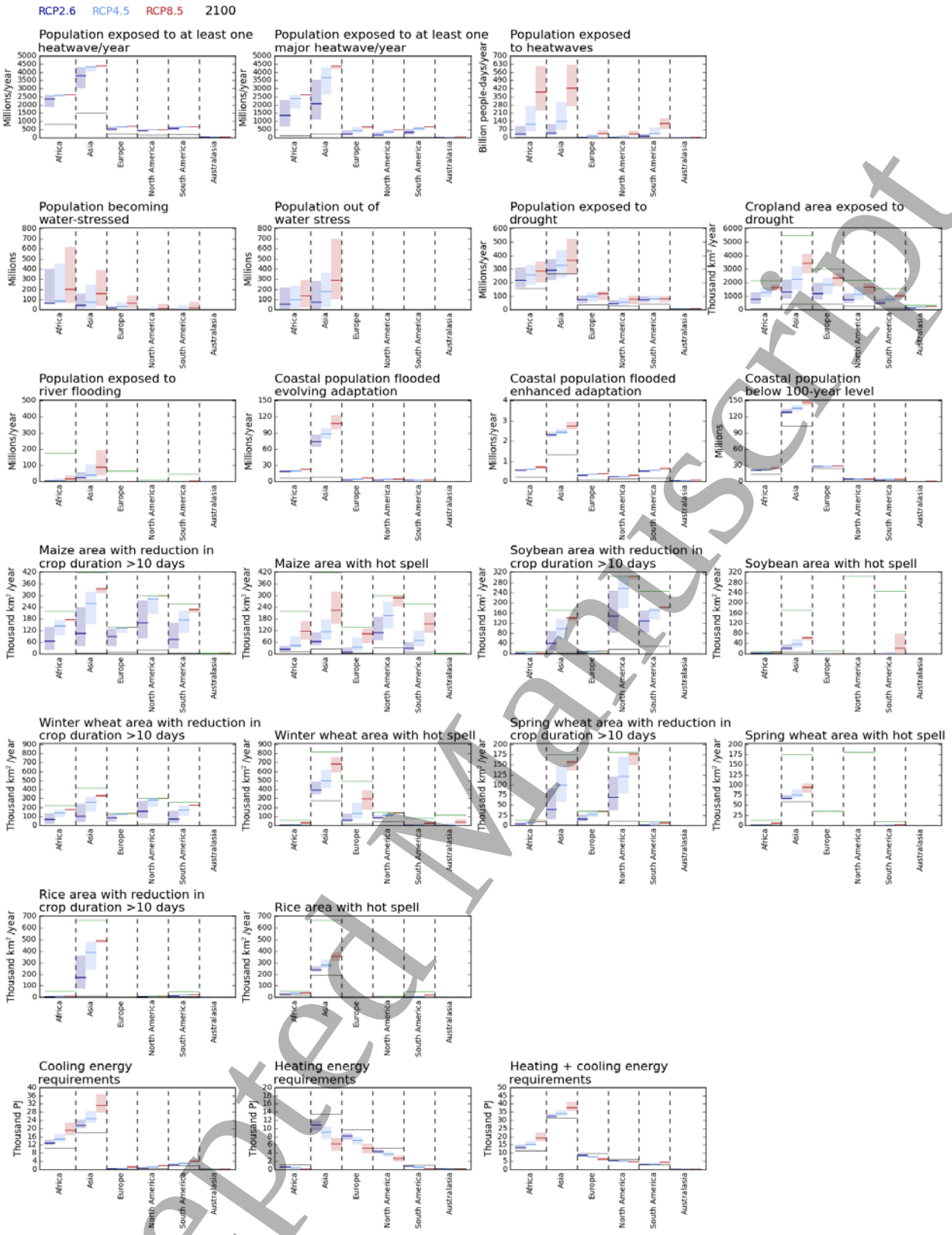

Figure 8: Impact indicators for each continent in 2100: RCP2.6, RCP4.5 and RCP8.5. SSP2 socio-economic scenario for the population indicators. The solid line represents the median and the shaded area the range between the 10th and 90th percentiles ("low" and "high" for the coastal indicator). For the cropland indicators, the green lines show the total regional cropland area, and for the river flood indicator the green line shows the total regional river floodplain population.

Accepted Manuscript

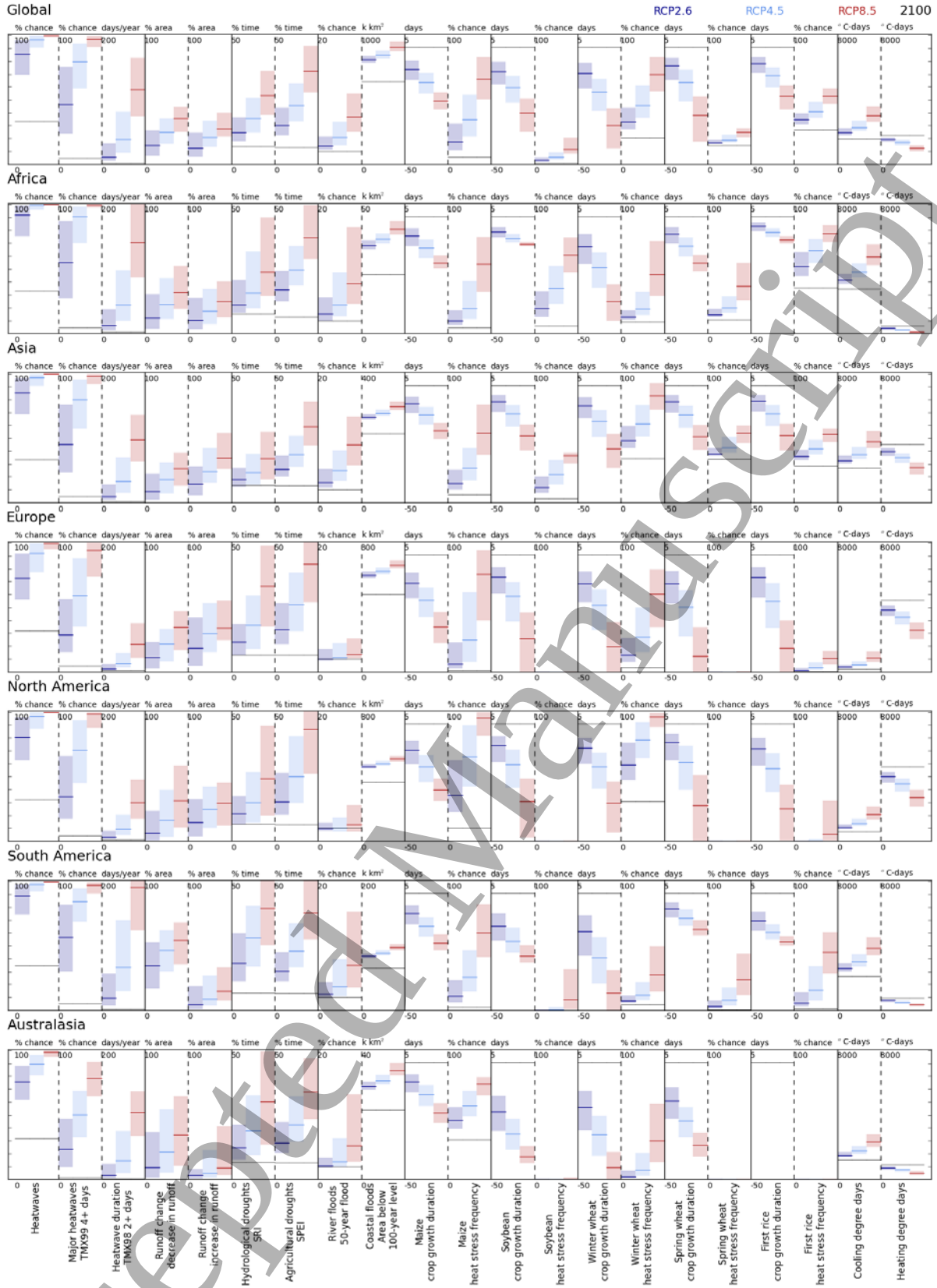

Figure 9: Overview of continental hazard indicators: 2100: RCP2.6, RCP4.5 and RCP8.5. The solid line represents the median and the shaded area the range between the 10th and 90th percentiles ("low" and "high" for the coastal indicator). The axis limits for each indicator are shown at the top of each column. The axis limits vary across continents.
the limits are the total regional continental cropland area, and for the river flood indicator the limits are the total regional river floodplain population.

Accepted Manuscript

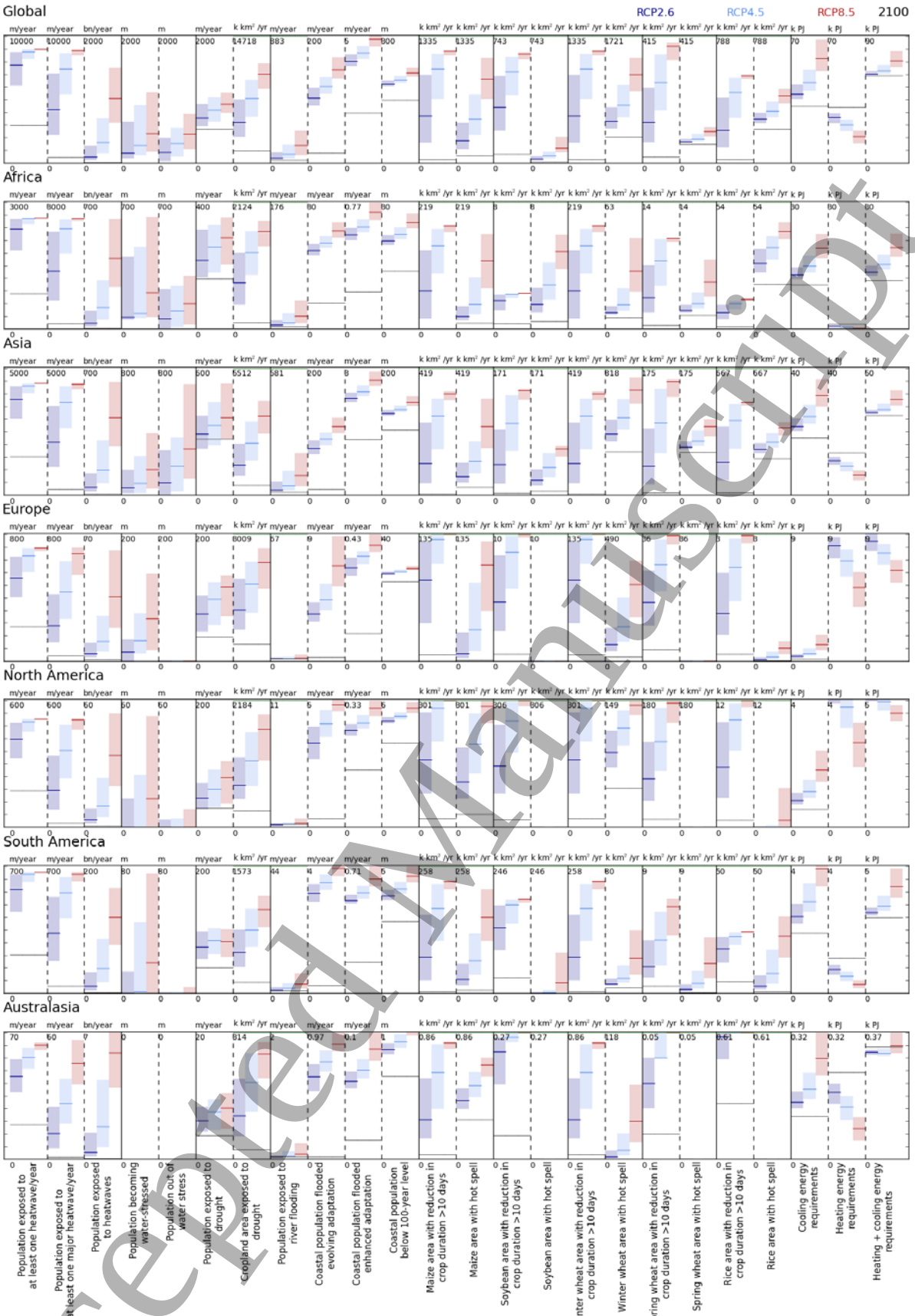

Figure 10: Overview of continental impact indicators: 2100: RCP2.6, RCP4.5 and RCP8.5. SSP2 socio-economic scenario for the population indicators. The solid line represents the median and the shaded area the range between the 10th and 90th percentiles ("low" and "high" for the coastal indicator). The axis limits for each indicator are shown at the top of each column. The axis limits vary across continents. For the cropland indicators the limits are the total regional continental cropland area, and for the river flood indicator the limits are the total regional river floodplain population.

Accepted Manuscript